

Anthrax Toxin: Receptor Binding, Internalization, Pore Formation, and Translocation

John A.T. Young¹ and R. John Collier²

¹Infectious Disease Laboratory, The Salk Institute for Biological Studies, La Jolla, California 92037; email: jyoung@salk.edu

²Department of Microbiology and Molecular Genetics, Harvard Medical School, Boston, Massachusetts 02115; email: jcollier@hms.harvard.edu

Annu. Rev. Biochem. 2007. 76:243–65

First published online as a Review in Advance on March 2, 2007

The *Annual Review of Biochemistry* is online at biochem.annualreviews.org

This article's doi:
10.1146/annurev.biochem.75.103004.142728

Copyright © 2007 by Annual Reviews.
All rights reserved

0066-4154/07/0707-0243\$20.00

Key Words

Brownian ratchet, proton gradient, self-assembly, receptor

Abstract

Anthrax toxin consists of three nontoxic proteins that self-assemble at the surface of receptor-bearing mammalian cells or in solution, yielding a series of toxic complexes. Two of the proteins, called Lethal Factor (LF) and Edema Factor (EF), are enzymes that act on cytosolic substrates. The third, termed Protective Antigen (PA), is a multifunctional protein that binds to receptors, orchestrates the assembly and internalization of the complexes, and delivers them to the endosome. There, the PA moiety forms a pore in the endosomal membrane and promotes translocation of LF and EF to the cytosol. Recent advances in understanding the entry process include insights into how PA recognizes its two known receptors and its ligands, LF and EF; how the PA:receptor interaction influences the pH-dependence of pore formation; and how the pore functions in promoting translocation of LF and EF across the endosomal membrane.

Contents

INTRODUCTION.....	244	INTERNALIZATION AND TRAFFICKING OF TOXIN-RECEPTOR COMPLEXES.....	252
STRUCTURES OF NATIVE PA AND THE HEPTAMERIC PREPORE.....	245	CONVERSION OF THE PA ₆₃ PREPORE TO THE PORE.....	252
Native PA: PA ₈₃	246	pH-Dependence and Mechanism of Pore Formation.....	253
The Heptameric PA ₆₃ Prepore....	246	Receptor Dependence of Pore Formation.....	254
ANTHRAX TOXIN RECEPTORS.....	247	Mutations in PA that Affect Pore Formation and Translocation ..	255
Two Receptors: ANTXR1 and ANTXR2.....	247	TRANSLOCATION OF LF/EF THROUGH THE PORE.....	255
Binding of PA to its Receptors....	247	pH-Dependent Unfolding of LF/EF.....	255
PROTEOLYTIC ACTIVATION OF PA AND OLIGOMERIZATION OF PA ₆₃	249	Translocation Is N to C Terminal .	256
Furin Cleavage and Release of PA ₂₀	249	A Transmembrane Proton Gradient Drives Translocation .	257
Self-Association of PA ₆₃	250	The Phenylalanine Clamp and Its Role in Translocation.....	258
Association of Toxin-Receptor Complexes with Lipid Rafts....	250		
BINDING OF LF AND EF TO THE PA ₆₃ PREPORE.....	251		
The Stoichiometry of Binding....	251		
The LF/EF Binding Site on PA ₆₃ ..	251		

Binary toxin: a toxin in which two compounds (proteins in this context) combine to elicit a toxic response

Lethal factor (LF): a Zn²⁺ protease that cleaves and inactivates most MAP kinase kinases

Edema factor (EF): a Ca²⁺- and calmodulin-dependent adenylate cyclase

Protective antigen: the transport protein of anthrax toxin, which combines with LF and/or EF to form toxic complexes

INTRODUCTION

Pathogenic bacteria have evolved a variety of ways to disable cells of the mammalian immune system in order to create a niche in which they can multiply and disseminate. Among the most interesting ways, from a biochemical perspective, is for the bacteria to release toxic proteins that are capable of penetrating to the cytosol of host cells and enzymically modifying key substrates within that compartment. This mode of action necessitates that the toxin, or at least an enzymically active piece of it, penetrate a host-cell membrane at some level. How this occurs is not fully understood for any toxin, but for some, including anthrax toxin, there has been significant progress recently [for recent reviews of this and related subjects, see (1–6)].

Anthrax toxin belongs to a family of toxins, called binary toxins, that are produced by

certain *Bacillus* and *Clostridium* species (7). Each binary toxin consists minimally of two nontoxic proteins that combine at the surface of a receptor-bearing eukaryotic cell or in solution to form toxic complexes. One of these proteins is an enzyme (the A moiety), and the other is a receptor-binding and pore-forming protein (the B moiety). *Bacillus anthracis*, the causative agent of anthrax, secretes three monomeric, plasmid-encoded proteins that are collectively called anthrax toxin. Two are enzymes: Lethal Factor (LF; 90 kDa), a Zn²⁺ protease that specifically cleaves and inactivates MAP kinase kinases (8, 9), and Edema Factor (EF; 89 kDa), a Ca²⁺- and calmodulin-dependent adenylate cyclase (10). The third, Protective Antigen (PA₈₃; 83 kDa), named for its effectiveness in inducing protective immunity against anthrax, is the vehicle for delivery of LF and EF to the cytosol.

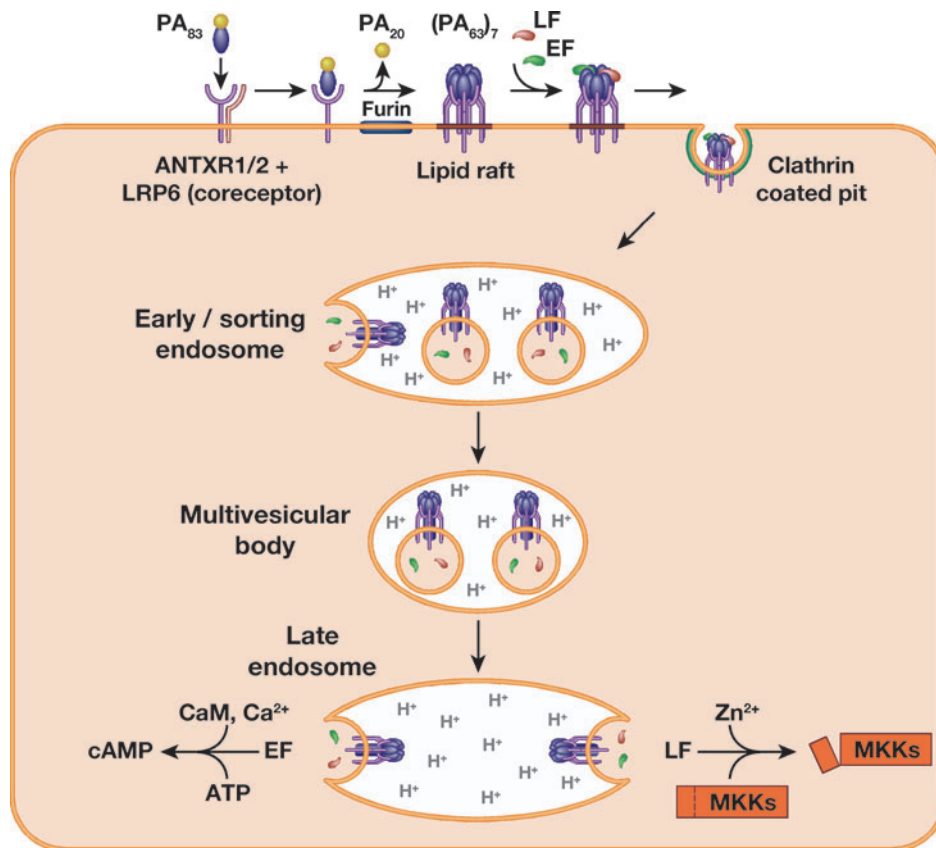


Figure 1

Entry of anthrax toxin into cells.

The following general model of anthrax toxin action at the cellular level has emerged in recent years (**Figure 1**). Toxin action begins when PA_{83} binds to either of two known receptors and is proteolytically activated by a member of the furin family of cellular proteases. This cleavage removes a 20-kDa piece (PA_{20}) from the N terminus, leaving the complementary 63-kDa piece (PA_{63}) bound to the receptor. Receptor-bound PA_{63} then self-associates to form a ring-shaped heptameric complex—the prepore—that is capable of binding up to three molecules of LF and/or EF competitively. Because each bound ligand molecule effectively occludes two subunits, only three ligand molecules can bind to the heptamer simultaneously. The resulting complexes are endocytosed and delivered to

an endosomal compartment. There, under the influence of low pH, the prepore forms a pore in the bounding membrane, initiating translocation of LF and EF to the cytosolic compartment. The cargo molecules are believed to unfold, partially or completely, in order to pass through the narrow (~ 15 Å) pore and therefore must refold in the cytosolic compartment to become enzymically competent.

STRUCTURES OF NATIVE PA AND THE HEPTAMERIC PREPORE

The crystallographic structure of native PA has defined its folding domains and provided the basis for analyzing its multiple functions. The structure of the heptameric PA_{63}

Prepore: a heptameric form of PA_{63} formed by spontaneous self-association; binds seven molecules of receptor and up to three molecules of LF and/or EF

prepore serves as a model of an important intermediate, which is capable of binding EF and LF and forming the transmembrane pore that translocates them to the cytosol.

Native PA: PA₈₃

A 2.1 Å crystallographic model of monomeric PA (PA₈₃; 83 kDa; 735 residues) shows a long, flat molecule of dimensions ~100 × 50 × 30 Å, containing four folding domains (11) (Figure 2).

Domain 1 (residues 1–258) consists of a β-sandwich with jelly-roll topology, four small

helices, and two calcium ions. Proteolytic activation by furin occurs at the sequence RKKR (residues 164–167) within a surface loop, generating a nicked form of PA₈₃ (nPA₈₃) as the precursor of the heptameric PA₆₃ prepore.

Domain 2 (residues 259–487) consists of a β-barrel core with elaborate excursions and a modified Greek-key topology. The major function of this domain is to form a transmembrane pore to serve as the portal of entry of EF and LF into the cytosol. Recently, domain 2 has also been shown to participate in binding PA₈₃ to cellular receptors (12, 13). In order to insert stably into membranes, PA₆₃ must oligomerize to the heptameric state, forming the prepore, and domain 2 must undergo a major pH-dependent conformational rearrangement. This allows the seven domains 2 to combine to form a 14-strand transmembrane β-barrel. The large 2β2–2β3 loop of domain 2, which is disordered in the monomer, forms the transmembrane portion of this β-barrel (14, 15).

Domain 3 (residues 488–595) has a ferridoxin-like fold and is believed to mediate self-association of PA₆₃. Mutations in a loop (residues 510–518) of this domain strongly inhibit oligomerization by PA₆₃, and the structure of the heptameric PA₆₃ prepore reveals that this loop inserts into a cleft in domain 1' of the adjacent subunit (residues 192–205) (12, 16).

Domain 4 (residues 596–735) consists primarily of a β-sandwich with an immunoglobulin-like fold and is primarily involved in binding to cellular receptors. This domain has relatively little contact with the rest of the protein (17).

The Heptameric PA₆₃ Prepore

A 4.5 Å structure of the water-soluble PA₆₃ heptamer (11), and a later 3.6 Å structure (12), show a hollow ring, 160 Å in diameter and 85 Å high, with the subunits packed like pie wedges. There are no major conformational changes from the structure of monomeric PA₈₃. Domains 1' and 2 are on the inside of the

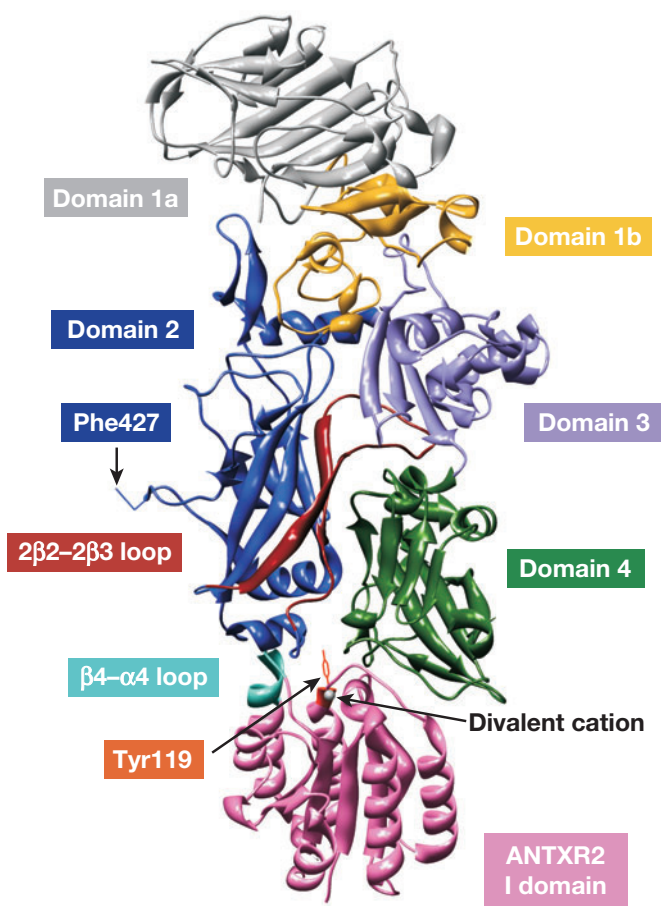


Figure 2

Monomeric PA complexed with the ANTXR2 I domain. This figure is adapted from PTBIT6B (13). The divalent cation bound to the receptor MIDAS is shown as a gray circle.

ring, and domains 3 and 4 are on the outside. The subunit:subunit interface is comprised mainly of charged or polar residues from domains 1' and 2. The lumen averages ~ 35 Å in diameter, narrowing to ~ 20 Å in places, and is lined mainly with polar and negatively charged amino acids. A conserved phenylalanine (Phe427) in a mobile, solvent-exposed loop in the lumen is a prominent exception, and as described below; this residue plays a major role in protein translocation through the pore (18).

Two other functionally important features of the prepore are a large, flat hydrophobic surface exposed on domain 1' at the top of the structure, which serves as the binding site for LF and EF, and the $2\beta 2$ – $2\beta 3$ loop of domain 2, which is involved in pore formation. Whereas the $2\beta 2$ – $2\beta 3$ loop is disordered in PA₈₃, the 3.6 Å structure of the prepore shows this loop to project outward, away from the monomer, and to be packed between domains 2 and 4 of the neighboring monomer (12). This implies that domains 2 and 4 must move apart during pore formation, a transition that involves a major structural rearrangement and relocation of the $2\beta 2$ – $2\beta 3$ loop.

ANTHRAX TOXIN RECEPTORS

Cell biological and molecular genetic studies have revealed the existence of two related cellular receptors for PA, both of which are capable of mediating anthrax toxin action. Many aspects of their interaction with PA₈₃ and the prepore are now understood, to the level of crystallographic detail for one of the receptors.

Two Receptors: ANTXR1 and ANTXR2

Two related cell surface receptors that bind PA₈₃ have been identified: ANTXR1 (tumor endothelial marker-8) and ANTXR2 (capillary morphogenesis protein 2) (**Figures 2 and 3**) (19, 20). Alternative mRNA splicing gives rise to three different protein isoforms

of each receptor. The long (564 amino acids) and medium-length (368 amino acids) forms of ANTXR1, and the long (489 and 488 amino acids) forms of ANTXR2, are type 1 membrane proteins that function as anthrax toxin receptors (19–22). By contrast, the short forms of these proteins (333 amino acids for ANTXR1, and 368 amino acids for ANTXR2), lack this function (21, 22). PA₈₃ binds to an approximately 190 amino acid-long extracellular domain of ANTXR1 and ANTXR2, which is related to von Willebrand factor type A (VWA) domains and integrin inserted (I) domains. The cytoplasmic tails of these receptors do not play a critical role in toxin entry since this region of ANTXR1 can be removed without abrogating intoxication (21).

Both ANTXR1 and ANTXR2 appear to be ubiquitously expressed and bind collagen $\alpha 3$ (VI) and collagen IV/laminin, respectively (23, 24). Both receptors are also expressed in vein endothelial cells where they appear to have important roles in regulating angiogenic processes (23–30). Mutations in the ANTXR2 gene are linked to two human autosomal recessive diseases, juvenile hyaline fibromatosis and infantile systemic hyalinosis (31, 32).

Binding of PA to its Receptors

PA₈₃ binds the soluble ANTXR2 I domain (residues 35–225) at a 1:1 ratio, as shown by isothermal titration calorimetry and by FRET (fluorescence resonance energy transfer)-based assays performed with an AF488 (donor fluorophore)-labeled version of PA₈₃ and an AF546 (acceptor fluorophore)-labeled version of the soluble ANTXR2 I domain (33) and by crystallography (**Figure 2**) (13). The heptameric PA₆₃ prepore can bind up to 7 molecules of the receptor I domain, as shown by the same FRET-based assay and by X-ray crystallography (**Figure 3**) (12, 33). Receptor binding does not influence the rate of PA₆₃ heptamer formation in solution (33).

ANTXR1 and ANTXR2: anthrax toxin receptors 1 and 2, respectively, the only known types of receptor for this toxin

VWA or I domain [von Willebrand Factor A, or integrin inserted (I) domain]: adopts a Rossman fold structure

FRET: fluorescence resonance energy transfer

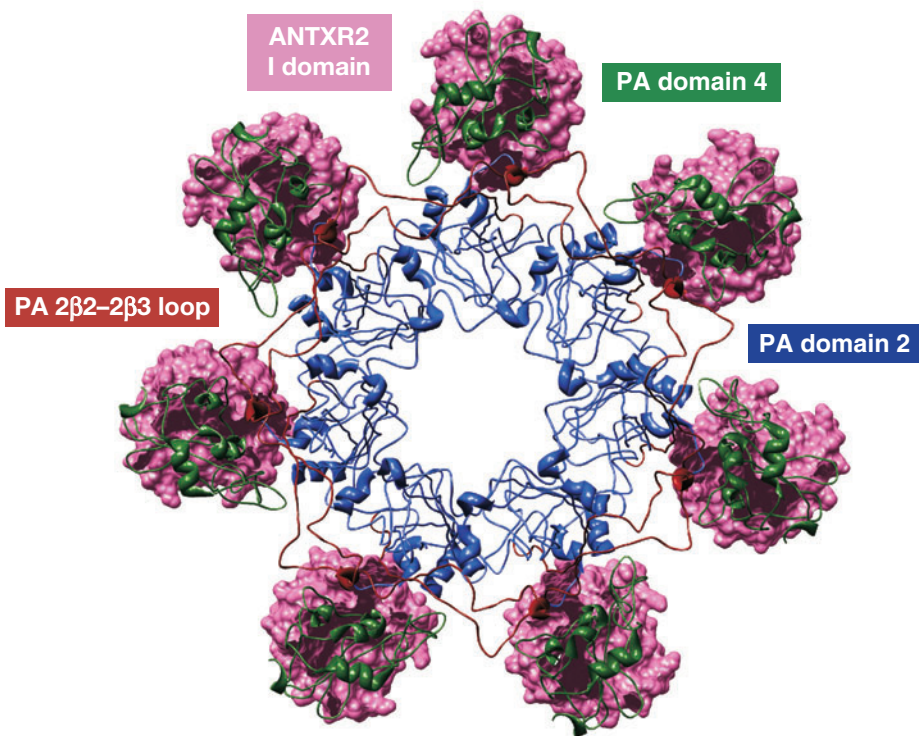


Figure 3

Top-down view of Protective Antigen (PA) domains 2 and 4 complexed with the ANTXR2 I domain. This figure is adapted from PDB 1TZN (12).

Like other VWA/I domains, those of ANTXR1 and ANTXR2 contain a metal ion-dependent adhesion site (MIDAS), which, in the anthrax toxin receptors, comprises residues Asp50, Ser52, Ser54, Thr118, and Asp148 (ANTXR2)/Asp150 (ANTXR1) (19, 20). The receptor MIDAS coordinates a divalent cation, which plays a role in PA-receptor binding (12, 13, 33, 35, 37).

PA-receptor interactions bear some similarity to those of I domain-containing α -integrins and their natural ligands. Integrin I domains can exist in either of two conformations, closed (low-affinity ligand-binding state) or open (high-affinity ligand-binding state) (36). Conversion from closed to open states requires the following: rearrangement of the MIDAS residue-metal ion contacts; metal ion coordination by a carboxylate-containing amino acid side chain of the bound ligand; movement of two conserved phenylalanines that bind within I-domain hydrophobic pockets; and a 10 Å downward movement of the C-terminal

α -helix of the I domain away from the MIDAS-containing face (36). The metal ion-coordinating residues in the PA-ANTXR2 I domain complex are arranged in an open configuration, with PA residue D683 and the receptor's MIDAS threonine and both MIDAS serines located within the primary metal ion coordination sphere (13, 34). Consistently, both receptor MIDAS aspartate residues are located in the secondary coordination sphere, where they bind the metal ion indirectly via water molecules (12, 13). The placement of the conserved ANTXR2 residues, Phe181 and Phe203, and of the C-terminal α -helix of the I domain in the PA-ANTXR2 complex is also consistent with an open conformation (12, 13, 34). In the case of ANTXR1, an open I-domain conformation appears to be essential for PA binding, since this interaction was abolished by substituting either the receptor MIDAS threonine or PA residue Asp683 (17, 35). However, although probably optimal for PA binding, such a conformation is not absolutely essential for ANTXR2; that receptor,

MIDAS: metal ion-dependent adhesion site

unlike ANTXR1, can bind and support intoxication mediated by D683N or D683K mutant forms of PA (37). Indeed, the D683K mutant form of PA can also mediate lethal toxin killing of Fischer 344 rats, albeit severalfold less efficiently than wild-type PA, indicating that ANTXR2 plays an important role in lethal toxin killing in vivo (37).

The PA-binding affinities of the ANTXR1 and ANTXR2 I domains are strikingly different from each other. The affinity of ANTXR1 [$K_D = 1.1 \mu\text{M}$ or 130 nM for the Mg^{2+} - and Ca^{2+} -bound complexes, respectively; (38)] is on a par with those of integrin-ligand interactions (36), but that of ANTXR2 is approximately 1000-fold higher ($K_D = 170 \text{ pM}$ or 780 pM for the Mg^{2+} - and Ca^{2+} -bound complexes, respectively) (33). Consistent with its higher binding affinity, the soluble ANTXR2 I domain is the more effective receptor decoy-based inhibitor of anthrax intoxication (38).

X-ray structural studies revealed why PA binds ANTXR2 with such high affinity. Compared to the 1300 \AA of buried protein surface that is typically associated with α -integrin-ligand interactions, there is $1900\text{--}2000 \text{ \AA}$ of buried protein surface at the PA-ANTXR2 interface, involving I domain contact with PA domain 4 and with the 340–380 loop of PA domain 2 (Figure 2) (12, 13). Homolog-scanning mutagenesis studies have subsequently revealed that receptor residues located in the $\beta 4\text{--}\alpha 4$ loop region of the I domain, which is involved in binding PA domain 2, contribute to the difference in PA-binding affinity between ANTXR1 and ANTXR2 (37).

The high binding affinities seen with the PA-ANTXR2 interaction in the presence of the metal ions are primarily due to very slow dissociation rates: $9.2 \times 10^{-6} \text{ s}^{-1}$ (Mg^{2+}) or $8.4 \times 10^{-5} \text{ s}^{-1}$ (Ca^{2+}) (33). Although the slow rate of PA dissociation from ANTXR2 is not commonly seen with other VWA domain-ligand interactions, it is also a feature of hookworm neutrophil inhibitory factor (NIF) binding to CD11b (39). Given the high binding affinity that exists between PA and its re-

ceptors, especially ANTXR2, it seems likely that PA binding could interfere with the association between these receptors and their physiological ligands. If so, disruption of these receptor-ligand interactions might also play a role in anthrax pathogenesis, an idea that remains to be formally tested.

PROTEOLYTIC ACTIVATION OF PA AND OLIGOMERIZATION OF PA₆₃

The proteolytic activation of native PA₈₃, which is effected in vivo by furin-family proteases, may be replicated in vitro with trypsin, allowing studies of the activation and the self-association of PA₆₃ to be performed in solution. These studies have been complemented by studies of the behavior of receptor-bound wild-type and mutated forms of PA in cultured cells.

Furin Cleavage and Release of PA₂₀

The N-terminal region of PA₈₃, corresponding to PA₂₀, sterically inhibits self-association of the protein and thus also blocks later steps in toxin action. To remove the blockage, receptor-bound PA₈₃ is cleaved by a furin-family protease (40, 41), generating a nicked form of the protein (nPA₈₃) that subsequently dissociates, releasing PA₂₀ into the medium. Dissociation of PA₂₀ (residues 1–167) from PA₆₃ requires a β -sheet to be ruptured and a large hydrophobic surface to be exposed. PA₂₀ and PA₆₃ tend to remain associated via non-covalent forces ($K_d \sim 190 \text{ nM}$) (42) and cofractionate on size-exclusion columns.

Domain 1', the segment of domain 1 that forms the N terminus of PA₆₃, generates the binding sites for EF and LF upon PA₆₃ oligomerization. Two calcium atoms are firmly bound within domain 1' ($t_{1/2}$ of exchange with free $\text{Ca}^{2+} \sim 4 \text{ h}$) and are thought to stabilize domain 1' in a conformation that facilitates oligomerization of PA₆₃ and binding of EF and LF (43). The dissociation rate constant of PA₂₀ and PA₆₃, k_{off} , has been

DRM:

detergent-resistant
membrane
microdomain

estimated by FRET measurements of dye-labeled fragments in solution to be $\sim 3 \times 10^{-2} \text{ s}^{-1}$ at 20°C, corresponding to a $t_{1/2}$ of 21 s (42). Thus, nPA₈₃ is largely dissociated within a minute after proteolytic activation, and dissociation is unlikely to be a rate-limiting step in toxin action, which occurs over tens of minutes at the cellular level. Dissociation of PA₂₀ from PA₆₃ in solution was also examined by stopped-flow FRET, and two steps were identified: a fast bimolecular step and a slower unimolecular step. The first step may correspond to dissociation of the PA₂₀:PA₆₃ complex and the second to an isomerization in the PA₆₃ moiety that could potentiate it for oligomerization and subsequent steps in toxin action.

Self-Association of PA₆₃

After PA₂₀ dissociates from nPA₈₃ it is free to diffuse in three dimensions, whereas receptor-bound PA₆₃ is constrained to diffuse in the two dimensions of the membrane. Effectively PA₆₃ therefore becomes concentrated relative to PA₂₀. Depending on a number of other factors, this could accelerate its self-association.

When PA₆₃ is purified from trypsin-activated PA₈₃ by anion-exchange chromatography, it is found to have spontaneously self-associated into a ring-shaped heptamer (44). As long as the pH is maintained above 8, the heptamer remains soluble, in the so-called prepore state. The association-dissociation equilibrium strongly favors the heptamer, and neither monomeric PA₆₃ nor subheptameric oligomers have been detected. Recent FRET measurements, performed with prepore prepared from PA preparations labeled with donor and acceptor fluorescent dyes, have yielded a dissociation rate constant, k_d , of $1 \times 10^{-6} \text{ s}^{-1}$, corresponding to a $t_{1/2}$ of ~ 7 days (45). In contrast, a ternary complex, containing the PA-binding domain of LF (LF_N) bound to a PA₆₃ dimer formed from two nonoligomerizing mutants, dissociated rapidly ($t_{1/2} \sim 1$ min). The remarkable stability of the prepore relative to the ternary complex presumably derives from each subunit

of the ring being bound to two neighboring subunits.

Association of Toxin-Receptor Complexes with Lipid Rafts

PA₆₃ oligomerization causes the receptors to cluster in detergent-resistant membrane microdomains (DRMs, or lipid rafts) (46). The precise nature of these DRMs is not known. However, PA₆₃ and antibody-clustered forms of PA₈₃ colocalize with GPI-anchored proteins, but not with caveolin-1, indicating that they are not caveolae (46). Consistently, PA₆₃ can form pores and can internalize LF in cells without caveolae (46).

Lipid-raft association is regulated by S-palmitoylation of the receptors. Residues Cys347 and Cys481 of the long isoform of ANTXR1 have been identified as major sites of S-palmitoylation, and residue Cys521 of this protein is a minor palmitoylated residue (47). A mutant receptor lacking all possible S-palmitoylation sites localizes constitutively to DRMs, indicating that this posttranslational modification negatively regulates receptor association with DRMs in the absence of PA binding (47). DRM association of this mutant receptor remained sensitive to inhibition by the palmitoylation inhibitor, 2-bromopalmitate, implicating the involvement of another palmitoylated protein in targeting the toxin-receptor complex to DRMs (47).

Oligomerization of PA and its clustering in lipid rafts are important for the subsequent internalization of PA:receptor complexes into cells. A furin-resistant PA mutant (PA^{SSSR}) was found to remain at the cell surface (48), and another such mutant (PA^{SNKE}) was internalized into CHO cells only after antibody-induced clustering (46). Moreover, antibody-induced clustering and internalization of wild-type PA₆₃, and LF translocation, were blocked by β -methylcyclodextrin (MCD) treatment, which extracts cholesterol from membranes, disrupting DRMs (46). It has been proposed that the slow intrinsic receptor internalization rate, and the rapid

uptake after heptamerization and LF/EF binding, help to facilitate intoxication (46).

BINDING OF LF AND EF TO THE PA₆₃ PREPORE

The availability of PA₆₃ prepore and its enzymic ligands in pure form, and the ability to prepare mutated forms of these proteins easily, have permitted the formation of toxic, heterooligomeric complexes to be examined in solution. While no crystallographic structure of such a complex has been reported, other approaches have yielded a detailed model of how the prepore binds these ligands.

The Stoichiometry of Binding

LF, EF, and LF_N bind to PA₆₃ with high affinity ($K_d \sim 1\text{--}2$ nM; $k_{on} \sim 3 \times 10^5$ M⁻¹ s⁻¹; $k_{off} \sim (3\text{--}5) \times 10^{-4}$ s⁻¹), as shown by surface plasmon resonance measurements with the purified proteins and by binding studies on L6 cells with radiolabeled forms of these proteins (49). LF and EF compete for the same sites on the PA₆₃ heptamer, and a single heptamer can bind both of these proteins simultaneously (50). Even though the heptameric PA₆₃ prepore has radial sevenfold symmetry, measurements by two independent methods showed that the heptamer binds only three molecules of ligand under saturating conditions (51). Later studies revealed that neither of two different oligomerization-deficient PA mutants, with lesions on different subunit:subunit contact surfaces, bound ligand; but a mixture of the two mutant proteins did (52). Mixing the two mutant forms of proteolytically activated PA with LF_N in solution yielded a ternary complex containing a single copy of each of these proteins. Thus, two molecules of PA₆₃ must come together to form a high-affinity LF/EF binding site. A mutagenesis study (53) confirmed that the ligand binding site spans the intersection between two PA₆₃ subunits, and further, that a single ligand molecule would be expected to occlude the binding sites of two subunits. This explained the finding

that the PA₆₃ heptamer binds a maximum of three ligand molecules. The saturated heptamer is therefore asymmetric, with six of the seven subunits blocked and the remaining one free. At variance with this picture, a study by cryoelectron microscopy of binding of LF to the PA₆₃ heptamer yielded results suggesting that a single molecule of LF interacts with four successive PA₆₃ monomers within the prepore and partially unravels the heptamer (54).

The LF/EF Binding Site on PA₆₃

Although no crystallographic model of the binding of EF or LF to PA₆₃ has been reported, directed mutagenesis and other methods have revealed how the binding domains of these ligands dock onto the PA₆₃ heptamer. Substitution of Ala for residues of LF_N that were selected from the crystallographic structure of LF, based on a sequence comparison with EF, allowed the face of this domain that recognized PA₆₃ to be identified (55). When Cys residues were introduced into this face and the binding surface of PA₆₃, three contact points were identified by disulfide cross-linking; and two additional contact points were found by directed charge-reversal mutations (56). These contact points were consistent with the lowest energy LF_N-PA complex by computational protein-protein docking with the Rosetta program. Enhanced peptide amide hydrogen/deuterium exchange mass spectrometry, and the demonstration that residues within this surface interact with Lys197 of two adjacent PA subunits simultaneously, allowed the PA-interactive surface on LF_N to be defined more precisely (57). The resulting model showed that EF and LF bind through a highly electrostatic interface, with their disordered, charged N termini poised at the entrance of the heptameric prepore, and thus positioned to initiate translocation in an N- to C-terminal direction.

The way in which EF and LF bind to PA₆₃ has ramifications for how these proteins affect the kinetics of assembly of heterooligomeric toxin complexes. Oligomerization of PA₆₃

in solution is accelerated by concentrations of LF_N up to 50 nM, but is inhibited at higher concentrations (45). A prepore liganded with LF/EF contains both liganded and unliganded PA₆₃ subunits, and of those subunits that are liganded, there exist two subpopulations, each with different contacts with the ligand. High concentrations of LF/EF can be conceived to inhibit oligomerization by fostering conversion of PA₆₃ to a liganded PA₆₃ dimer, thereby depleting free PA₆₃, which is necessary to form a complete prepore. Alternatively, the inhibition could result from weak interactions of LF/EF with PA₆₃ monomers, yielding a population of heterodimers that is biased toward one of the two subpopulations of ligand:PA₆₃ interactions within the liganded heptamer.

INTERNALIZATION AND TRAFFICKING OF TOXIN-RECEPTOR COMPLEXES

Following lipid-raft association, anthrax toxin-receptor complexes are believed to be internalized primarily through clathrin-coated pits and then trafficked to early endosomes. Supporting this model, antibody-cross-linked forms of PA₈₃ colocalize with clathrin-coated pits and vesicles early after internalization and expression of the dominant-negative EΔ95/295 form of Eps15, which specifically interferes with clathrin-mediated endocytosis and blocks internalization (46). However, other cellular endocytic pathways have also been implicated in toxin uptake (58).

Anthrax toxin uptake is dependent upon ubiquitination of a conserved receptor lysine residue (Lys352 in ANTXR1 and Lys350 in ANTXR2), mediated by the cellular E3 ligase Cbl (47). The cell surface protein LRP6 is also involved, acting as a toxin coreceptor (59). The extracellular domain of LRP6 interacts, either directly or indirectly, with ANTXR1 and ANTXR2 in a PA-independent manner. This coreceptor stimulates PA-binding as well

as toxin internalization, and the latter property requires the LRP6 cytoplasmic tail (59).

LRP6 is a component of cellular Wnt-signaling pathways, associating with Wnt ligands and the frizzled receptors, and it can downregulate this pathway by regulating internalization of LRP6/Kremen(Krm)/Dickkopf (DKK) complexes (60). It remains to be seen if additional Wnt-signaling components are associated with LRP6-ANTXR1/ANTXR2 complexes. LRP6 appears to play a very specific role in toxin entry, since the highly related LRP5 protein, which also functions in Wnt-signaling, does not appear able to functionally substitute for LRP6 in anthrax toxin internalization (59). LRP6-specific antibodies interfere with anthrax intoxication, indicating that this newly identified coreceptor might be a viable target for the development of novel antitoxins (59).

ARAP3, a phosphoinositide-binding protein with two GTPase activating (GAP) domains, one for ARF6 GTPase and another for Rho GTPase (61), also plays a role in toxin uptake after PA-receptor binding (62). Because ARF6 recruits clathrin adaptor protein 2 (AP2) and clathrin to coated pits (63, 64), it seems likely that ARAP3 impacts clathrin-dependent endocytosis of the toxin-receptor complexes. However, the precise role of ARAP3 in anthrax toxin internalization remains to be determined. Following internalization, the toxin-receptor complexes are trafficked to an early endosomal compartment containing Rab5, a small GTPase regulatory protein involved in sorting endosome formation and function (65, 66).

CONVERSION OF THE PA₆₃ PREPORE TO THE PORE

The conformational transition of the PA₆₃ prepore to the pore has been shown to be dependent both on acidic pH and the specific receptor to which it is bound. Mutational analysis of PA and its receptors has yielded insights into the mechanism by which receptors

influence the pH threshold of prepore-to-pore conversion.

pH-Dependence and Mechanism of Pore Formation

Addition of small amounts of trypsin-activated PA₈₃ or purified PA₆₃, but not native PA₈₃, to planar phospholipid bilayers or liposomes causes cation-selective channels (pores) to form (67–69). Channel formation was observed with membranes composed of asolectin or diphytanoyl phosphatidylcholine, and there have been no indications that channel formation or function depends on specific lipids. The rate at which PA₆₃ forms channels is accelerated by mild acidification of the *cis* compartment of planar bilayers (the compartment to which the protein was added). Consistent with this, one can demonstrate permeabilization of the plasma membrane of mammalian cells to ⁸⁶Rb⁺ and ²²Na⁺ by nPA₈₃ or PA₆₃ under acidic conditions (69). PA has also been shown to mediate the translocation across the plasma membrane of EF, LF, and fusion proteins derived from their N-terminal, PA₆₃-binding domains (70). This translocation is pH dependent, with a pH optimum of ~5.5. Consistent with these findings, PA₆₃ pore formation and translocation occur within acidic endosomal compartments (1, 22, 46). Recent findings in a liposomal system indicate that an important role of receptors is to favor partitioning of PA₆₃ into membranes by maintaining the prepore in close proximity to the target membrane, and presumably in an optimal orientation, when it undergoes pH-dependent conformation to the pore state (71). When the prepore is exposed to acidic pH in solution, it rapidly loses the ability to insert into membranes.

The crystallographic structures of PA₈₃ and the prepore revealed the 2β2–2β3 loop as a candidate for formation of a transmembrane 14-strand β-barrel similar to that seen in the pore formed by the α-toxin of *Staphylococcus aureus* (11). Evidence in favor of this model came from experiments in which pores

formed in planar lipid bilayers from PA mutants containing Cys substitutions in the 2β2–2β3 loop were exposed to the thiol-reactive probe, methanethiosulfonate ethyltrimethylammonium (MTS-ET) (14). Because reaction with this reagent adds a positively charged group, modification of those Cys residues with side chains projecting into the lumen would be predicted to inhibit conductance of the cation-selective pore. Conversely, Cys residues with side chains facing the lipid bilayer should be inaccessible to MTS-ET and thus should have no effect on conductance. The pattern of effects of MTS-ET observed coincided with that predicted by the β-barrel model. Thus, strong inhibitory effects were seen at alternating positions over two stretches corresponding to the descending and ascending strands of the putative β-barrel, and also at four consecutive residues corresponding to the turn region.

Additional support for this model of membrane insertion has come from studies *in vivo* with PA labeled at Cys residues in the 2β2–2β3 loop with the environment-sensitive fluorophore, 7-nitrobenz-2-oxa-1,3-diazole (NBD) (15). Membrane insertion was monitored in CHO cells by following the increase in fluorescence intensity of NBD as it entered the nonpolar environment of the bilayer.

Major conformational rearrangements of domain 2 are required for the 2β2–2β3 loops of the seven PA₆₃ subunits of the prepore to interact to form a 14-strand β-barrel. Because, in the prepore, the 2β2–2β3 loop is sandwiched between domains 2 and 4 of a neighboring subunit, these domains must move apart for the loop to be relocated to the base of the heptamer (12). In addition, because the 2β2–2β3 loop is part of a Greek key motif and extends laterally from approximately the vertical midpoint of domain 2, the flanking 2β2 and 2β3 strands must be stripped out of that domain for the relocation to occur (11).

In an extension of the original studies in planar bilayers, the approach of coupling MTS-ET inhibition of conductance with

Cys-scanning mutagenesis was applied to sequences flanking the 2 β 2–2 β 3 loop (72). The results suggest that the β -barrel structure extends well beyond the 2 β 2–2 β 3 loop and incorporates the 2 β 2 and 2 β 3 strands and the 2 β 1–2 β 2 and 2 β 3–2 β 4 loops. If residues 303–324 comprise the transmembrane region, as predicted, then the entire β -barrel, predicted to encompass residues 275–352, could be over twice as long as the 14-strand β -barrel of the α -hemolysin. A model of the PA₆₃ pore based on this information and energy minimization calculations has been published (73).

Receptor Dependence of Pore Formation

The crystal structures of ANTXR2-PA complexes revealed that this receptor acts as a molecular clamp, binding PA domains 2 and 4, to restrict toxin pore formation at neutral pH (12, 13). Indeed, the pH profile of PA₆₃ pore formation is consistent with titration of histidine residues in the toxin-receptor complex: There are 4 histidines in the 285–340 stretch of PA domain 2, and receptor residue His121, which is conserved in both ANTXR1 and ANTXR2, is located at the PA-binding interface (12, 13). Until recently, it was thought that prepore-to-pore conversion would occur under the same low-pH conditions if the toxin was bound to either ANTXR1 or ANTXR2. However, a striking 1.0 pH unit difference was found in the pH thresholds for pore formation when PA is bound to ANTXR1 (~pH 6.2) versus ANTXR2 (~pH 5.2) (22, 74). Multiple lines of evidence support this conclusion, including immunoblot and electrophysiological patch-clamp analyses, used to study PA₆₃ pore formation on cell surfaces; excimer fluorescence measurements of pyrene-labeled Asn306Cys PA-receptor complexes; and the fact that ANTXR2-dependent toxin entry is inhibited by the lysosomotropic agent ammonium chloride, whereas ANTXR1-dependent entry is not (22, 74). These findings raise the possibility that pore formation occurs within distinct endosomal compartments, depending upon whether the toxin is associated with

ANTXR1 or ANTXR2: the intraluminal pH of the sorting endosome is in the range of pH 5.9–6.0, whereas that of late endosomes is typically pH 5.0–6.0 (66). Given these findings, it will be of interest to determine whether PA₆₃ heptamers can form mixed complexes with both ANTXR1 and ANTXR2 and if so, to establish how differences in the ratios of these receptors in the complexes influence the pH threshold for toxin pore formation. Furthermore, although it was proposed that the receptor might remain bound to form a structural support for the newly formed pore (13), coimmunoprecipitation studies have failed to detect receptors associated with PA₆₃ pores, indicating that the receptors may be released (22). Indeed, pore formation in the absence of receptor binding is consistent with the fact that (PA₆₃)₇ pores can be formed in membranes that do not contain anthrax toxin receptors (67).

Mutational studies have identified the key determinants that distinguish the activities of the ANTXR1 and ANTXR2 clamps. The key regulator of acid pH-dependent pore formation was residue Tyr119. Replacement of this residue of ANTXR2 with either a Phe or an Ala led to a dramatic 0.6–0.8 shift in the pH threshold required for toxin pore formation (H. Scobie et al., submitted). It is not yet known why the hydroxyl moiety of this side chain, which is located at the binding interface with PA domains 2 and 4 (**Figure 2**), is so important for this process, although it is predicted to make H-bonds with the polypeptide backbone at PA residue Ala341 and/or with the Arg side chain of PA residue 659. Additionally, residues located in the β 4– α 4 loop region of the ANTXR2 I domain, which bind PA domain 2 (**Figure 2**), have been identified as major determinants of the 1.0 pH unit difference in the receptor-specific pH threshold of pore formation (H. Scobie et al., submitted). Together, these studies support a model in which toxin pore formation minimally involves receptor release of PA domain 2 and the neighboring edge of PA domain 4.

Mutations in PA that Affect Pore Formation and Translocation

Point mutations that strongly inhibit the translocation function of PA were identified by site-directed mutagenesis in two solvent-accessible loops of domain 2 (2 β 7–2 β 8 and 2 β 10–2 β 11), which lie on the luminal surface of this domain (75). Subsequently, a scan of the entire PA₆₃ fragment by Cys-replacement mutagenesis revealed a total of 33 sites at which the mutation inhibited toxin action at least 100-fold in cell culture (76). The fact that 22 of the 33 sites lie in domain 2 shows the remarkable sensitivity of this domain to mutational disruption. This sensitivity may reflect the major conformational rearrangements in domain 2 needed for pore formation and translocation.

Two classes of mutations in domain 2 have been characterized: (*a*) those that block conversion of the prepore to the pore, and (*b*) those that allow pore formation, but block the pore's ability to translocate its substrates (75, 77, 78). The first class is illustrated by replacements for Asp425, a residue in the 2 β 10–2 β 11 loop. The Asp425Ala mutation, for example, blocks the ability of PA to permeabilize the plasma membrane of CHO cells to ⁸⁶Rb⁺ and the ability to convert from the SDS-dissociable prepore to the SDS-resistant pore (75).

Some of the mutations in domain 2 that inhibited pore formation and/or translocation are dominantly negative (DN) (76–78). Thus, when heptameric prepores were formed from mixtures of mutated PA and wild-type PA, the mutated form strongly inhibited pore formation and/or translocation. Asp425Lys and Phe427Ala, both of which are in the 2 β 10–2 β 11 loop, exhibited strong dominant-negative properties, and other DN mutations have been identified in the nearby 2 β 6 and 2 β 7 strands, suggesting that this region of domain 2 undergoes significant reorganization during prepore-to-pore conversion. Some of the mutations that block pore formation and translocation are

not dominantly negative, however, such as Lys397Asp.

With the most strongly inhibitory of the DN mutants, the presence of a single mutant subunit within the prepore may be sufficient to ablate its activity, suggesting that DN forms of PA could be used as novel antitoxins (77, 78). Thus in an anthrax infection, injected DN-PA would coassemble with wild-type PA to yield inactive prepores or pores, preventing EF and LF from entering the cytosol. Furthermore, since the DN mutations tested did not impair immunogenicity of PA, the mutated proteins could also potentially induce a long-term protective immune response. Hence, DN-PA might represent a combination therapeutic and vaccine for anthrax. Initial experiments in the Fischer 344 rat model of lethal toxin action showed that substoichiometric amounts of either of two DN forms of PA, one with the Phe427Ala point mutation and another with two mutations, Lys397Asp and Asp425Lys, completely blocked the effects of a lethal combination of LF and PA.

TRANSLOCATION OF LF/EF THROUGH THE PORE

Among the many toxins that act by enzymically modifying cytosolic substrates, anthrax toxin has proven perhaps the most tractable to the study of the translocation process. Various approaches, but in particular electrophysiological measurements in planar phospholipids bilayers, have elucidated key features of translocation, including the role of the N terminus of EF and LF, the function of the PA₆₃ pore, and the energetics of translocation.

pH-Dependent Unfolding of LF/EF

By analogy with the staphylococcal α -hemolysin structure, the lumen of the putative 14-strand β -barrel formed by PA₆₃ is predicted to be ~ 15 Å in diameter. The β -barrel is lined principally by residues with small

Molten globule: a compact, partially folded state observed under mildly denaturing conditions, such as low pH; much of the original secondary structure is retained

side-chain volumes, such as Ser and Thr, and has been predicted by modeling to accommodate LF_N in an α -helical configuration (79). Thus, the β -barrel could accommodate α -helix or extended polypeptide, and larger structures would need to unfold in order to be translocated. Indeed, there is evidence that impediments to unfolding block translocation in this system (70). Fusions of LF_N with the catalytic domain of diphtheria toxin (DTA) or with dihydrofolate reductase (DHFR) were shown to be translocated by PA across the plasma membrane of CHO cells when the pH of the medium was lowered, but translocation was blocked either by introduction of an artificial disulfide bridge into the DTA moiety of LF_N-DTA or by adding a small-molecular-weight ligand of DTA (adenine) or DHFR (methotrexate) that stabilized the native conformation.

The low-pH conditions of the endosome can be conceived to facilitate unfolding of LF and EF as a prelude to their entry into the PA₆₃ pore, and the unfolding properties of the isolated N-terminal LF_N and EF_N domains in solution suggested that this may be the case (79). The pH-dependence of the unfolding of each of these domains was examined by fluorescence and circular dichroism in the presence and absence of chemical denaturants. Both proteins were shown to unfold via a four-state mechanism: $N \leftrightarrow I \leftrightarrow J \leftrightarrow U$, N being the native state, U the unfolded state, and I and J the intermediate states. The acid-induced $N \rightarrow I$ transition occurs over a pH range of pH 5–6, approximating the pH range of the endosome. The I state, which predominates at lower pH values, is compact and has the characteristics of a molten globule. The J and U states are populated significantly only in the presence of denaturant. Thus, the molten globular I state is the primary candidate as an intermediate in the unfolding process and in entry of EF and LF into the PA pore. Cellular studies performed with ammonium chloride revealed, however, that LF translocation can also occur under near-neutral pH levels in ANTXR1-expressing cells (22). The rate-

limiting step of entry has not yet been determined, and before the importance of the acid-induced unfolding of ligands can be determined, it will be important to measure the rates of various steps in this process as a function of pH.

LF and EF are believed to be delivered initially into the lumen of intraluminal vesicles within the endosomal pathway (65). These vesicles are then trafficked to late endosomes where they fuse with the limiting endosomal membrane, releasing the enzymatic toxin subunits into the cytosol (65). Consistent with this model, toxin delivery is impaired by nocodazole treatment, which disrupts trafficking of vesicles from early to late endosomes; by disruption of late endosome function through expression of the Asn125Ile dominant-negative form of Rab 5; by a lysobisphosphatidic acid (LBPA)-specific antibody that inhibits formation of these vesicles; and by knocking-down expression of ALIX, a homolog of the yeast class E vps31 protein, involved in multivesicular body (MVB) sorting and biogenesis (65). Also, electron microscopic analysis has confirmed that PA₆₃ pores are found on the membranes of these vesicles (65). Consistently, SDS-resistant PA₆₃ heptamer formation was blocked at the restrictive temperature in IdIF cells that harbor a temperature-sensitive defect in the epsilon COPI coatamer subunit that interferes with MVB formation (65). It has been proposed that this pathway of toxin delivery into cells may be required for the efficient interaction of LF with its MEK1 substrate, located within a scaffolding complex which is associated with late endosomes (65).

Translocation Is N to C Terminal

The crystallographic structure of LF revealed that the N-terminal 30 amino acids of LF_N comprise a disordered region containing a high density of acidic and basic residues (80). This flexible region is connected to a helix that extends outward from the main body of the domain and, according to the current model

of LF_N docked to the prepore, positions the flexible N terminus close to the mouth of the pore. N-terminal truncations of 27 or 36 residues strongly impaired acid-induced translocation of LF_N across the plasma membrane without significantly affecting its binding to PA₆₃ (81). The same truncations also ablated the protein's ability to block ion conductance of PA₆₃ pores formed in planar bilayers at a small positive voltage (+20 mV). Fusing a hexahistidine tag to the N terminus of the truncated proteins restored both translocation activity and channel-blocking activity. Also, at +20 mV, hexahistidine and biotin tags at the N terminus were accessible to Ni²⁺ and streptavidin, respectively, added to the *trans* compartment of a planar bilayer.

Taken together, these findings suggest that the N terminus of bound LF or EF enters the PA₆₃ pore under the influence of acidic pH and a positive membrane potential, and initiates translocation of the unfolded polypeptide in an N- to C-terminal direction. By protonating His and acidic residues, low pH is predicted to destabilize LF_N, give the N-terminal flexible region of LF and EF a net positive charge, and perhaps also attenuate the electrostatic component of the nM affinity of these proteins for oligomeric PA₆₃.

The role of a positively charged N terminus in initiating the threading of ligands into the PA₆₃ pore may explain the finding that fusing short tracts of cationic residues—Lys, Arg, or His—to the N terminus of DTA enabled this protein to be translocated to the cytosol by PA, causing the inhibition of protein synthesis (82). Lys₈DTA showed ~10% the activity of LF_NDTA and was the most effective of the tagged proteins tested. A high concentration (~1 mM) of a short synthetic peptide containing a Lys₆ tract gave measurable protection against the action of Lys₆DTA, but LF_N did not, even at saturating concentrations (1 μM). These findings suggest that the electrostatic attraction of a polycationic tag may be sufficient to guide a protein with no significant affinity for the LF/EF site on PA₆₃ into the prepore.

A Transmembrane Proton Gradient Drives Translocation

It is possible to measure translocation of PA₆₃ ligands, such as LF_N, across planar lipid bilayers by monitoring ion conductance, and this provides a means to address the question of what drives translocation in this system. LF_N enters the PA₆₃ pore at small positive voltages and blocks ion conductance (81, 83, 84). At large positive voltages it is translocated to the opposite side of the membrane, thereby unblocking the pore (84). Thus all of the translocation machinery is apparently contained in the PA₆₃ pore, and, at least in this system, translocation does not require cellular proteins or ATP. Using this *in vitro* system as a model of translocation across the endosomal membrane, one can investigate the applied transmembrane potential ($\Delta\Psi$) and a proton gradient (ΔpH) as potential sources of energy to drive translocation. When these two parameters were varied independently, translocation of LF_N and of full-length LF and EF was found to be markedly stimulated by ΔpH —that is, when the pH of the *trans* side of the membrane (corresponding to the cytosol) was greater than that of the *cis* side (corresponding to the endosomal lumen) (85). For example, at a low $\Delta\Psi$ of +20 mV no translocation of LF_N occurred at pH 5.5 if $\Delta\text{pH}=0$, whereas there was rapid translocation ($t_{1/2} \sim 10$ s) when the *trans* pH was raised to 6.2. Little translocation of whole LF or EF occurred at symmetric pH 5.5, even at a moderate $\Delta\Psi$ of +50 mV, but introduction of a ΔpH resulted in significant translocation. In comparing the $\Delta\Psi$ dependence of LF_N translocation in the presence and absence of a one-unit ΔpH ($\text{pH}_{\text{trans}} = 6.5$, $\text{pH}_{\text{cis}} = 5.5$), the ΔpH was better able to promote translocation at lower voltages than at higher voltages. Extrapolating the translocation $t_{1/2}$ back to 0 mV revealed that the ΔpH would accelerate translocation ~100-fold relative to that expected at symmetric pH. It is generally accepted that the sign of $\Delta\Psi$ across the endosomal membrane is positive (promoting passage

Brownian ratchet: in the current context, a mechanism of translocation across a membrane involving biased random thermal motion and driven by a chemical asymmetry between the two sides of the membrane

Phenylalanine clamp: a structure, formed by the seven Phe427 side chains within the PA₆₃ pore that is essential for translocation and is believed to interact directly with the translocating polypeptide

of cations from the *cis* to the *trans* compartment and anions in the opposite direction), but estimates of the magnitude of $\Delta\Psi$ vary widely (86–88). The translocation process in planar bilayers closely matches results seen *in vivo* when the applied $\Delta\Psi$ is small (0–20 mV), suggesting that the $\Delta\Psi$ across the endosomal membrane is within this range.

Taken together, these findings suggest that translocation across the endosomal membrane is driven primarily by the proton gradient, although $\Delta\Psi$ may play a role, particularly in the initial threading of the cationic N-terminal region through the pore to the cytosol. How might the proton gradient drive translocation? A charge-state Brownian ratchet mechanism has been proposed (85). The pore is cation selective (67); hence it disfavors the passage of anions and thus also of negatively charged segments of a translocating polypeptide. The relative rates of protonation and deprotonation of acidic side chains on the *cis* and *trans* sides of the membrane should thus bias Brownian fluctuations of the translocating polypeptide, driving the chain through the pore in a unidirectional manner. A stretch of anionic polypeptide can only enter the cation-selective portion of the pore after it is protonated and enough of the negative charge is neutralized to make the stretch neutral or cationic. As the stretch exits the pore and enters the higher pH of the *trans* compartment (cytosol), the acidic residues become deprotonated, giving the segment a negative charge and blocking back diffusion into the pore. The result is a unidirectional diffusion of the polypeptide across the membrane, accompanied by unfolding of the polypeptide as it is threaded into the pore and ultimately by refolding after it has emerged into the cytosol. Refolding would not be expected to be a significant driving force until relatively long segments of polypeptide had emerged from the pore, and experimental evidence supports this assumption (85). The extant data do not exclude the possibility that chaperonins, either endosomal or cytosolic, may play a role in translocation *in vivo*.

The Phenylalanine Clamp and Its Role in Translocation

What role does the PA₆₃ pore play in the translocation of EF and LF across the endosomal membrane? Recent studies indicate that the pore does not serve simply as a passive, water-filled conduit, but rather, actively catalyzes the passage of substrate proteins across the membrane. This conclusion derives primarily from studies of Phe427 of PA (18). Mutation of Phe427 to Ala was found to have a drastic inhibitory effect on the ability of PA to mediate translocation of LF_NDTA into cells. Indeed, this mutation was dominantly negative, although it did not block formation of pores in planar bilayers. In the crystallographic structure of the prepore, the seven Phe427 residues are seen to be luminal, near the base of the structure, and ~ 20 Å apart in neighboring subunits. Three lines of evidence indicate that these residues remain luminal and solvent-exposed when the prepore converts to the pore. (a) Single-channel ion conductance was diminished by replacing Phe427 with a bulkier residue, such as Trp, and increased by a less bulky residue, such as Ala. (b) When pores containing the Phe427Cys mutation were reacted with MTS-ET, a reagent that covalently links a positively charged group to the thiol, ion conductance was strongly inhibited. (c) When PA Phe427ys was reacted with a spin probe, the electron paramagnetic signature showed only weak spin-spin interaction in the prepore, but strong interaction in the pore. The data from the spin-spin interaction studies indicate that the Phe427 side chains come closer together, perhaps within 10 Å of one another, as the prepore converts to the pore.

How the Phe427 side chains are repositioned during prepore-to-pore conversion remains to be determined, but recent evidence suggests the existence of a scaffold in which an acidic residue, Asp426, immediately adjacent to Phe427, forms a salt bridge with a basic residue, Lys397, in an adjacent subunit of the pore (Figure 4) (89). While the members

of this salt bridge are conserved in other binary toxins produced by *Bacillus* species, both residues are Gln in Clostridial homologues of PA, indicating that hydrogen bonds replace ionic interactions in the Clostridial toxins.

When various amino acid replacements for Phe427 were tested for effects on the kinetics of translocation in the planar bilayer system, the results correlated well with the effects seen on toxin action in cultured cells (18). Phe at position 427 was most effective in promoting translocation, but Leu, Trp, and Tyr also showed strong activity. Ile was much less active than Leu, and Ala, Val, Val, Asp, Ser, and Gly were essentially completely inactive. Thus, the presence of a hydrophobic residue at position 427 is important in promoting translocation, but not just any hydrophobic residue will function, as both Ile and Val were virtually inactive. This suggests that a discrete structure involving Phe427 forms within the pore and that the structure is sensitive to small differences in side-chain structure at that position.

The results described indicate that the seven Phe427 residues form a structure in the lumen of the pore that facilitates translocation of LF and EF. Where is this structure located, and how does it facilitate translocation? The pattern of MTS-ET effects in the vicinity of position 427 appears to be inconsistent with Phe427 being in the 14-strand β -barrel of the pore, and it is thus in the cap region, perhaps near the proximal end of the β -barrel (18). Precisely how the Phe427 structure functions remains uncertain, but clues have come from planar bilayer studies. In single-channel measurements, LF_N is seen to produce a completely and continuously closed state of ion conductance. In contrast, with the Phe427Ala channel, LF_N produces a dynamic “flickering” between an open state, a fully closed state, and multiple partly closed substates. The simplest interpretation of these findings is that the wild-type Phe427 structure “clamps” the flexible N terminus of LF_N in such a manner that passage of hydrated K⁺ ions is prevented; hence, the term phenylalanine clamp (Phe

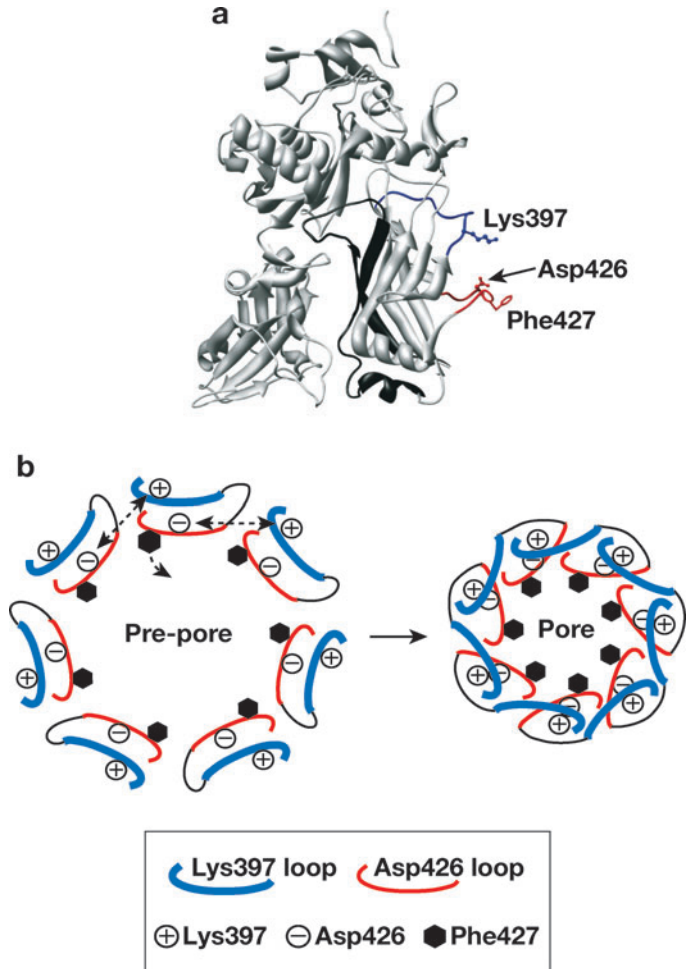


Figure 4

(a) Ribbon model of a PA₆₃ monomer, showing the locations of Lys397, Asp426, and Phe427. (b) Conceptual model of the formation of a scaffold for Phe427 in the PA₆₃ pore by the interaction of the Lys397 and Asp426 side chains. This figure is adapted from (89).

clamp or ϕ clamp) has been coined for the structure. With Ala at position 427, the substrate polypeptide is not stably bound within the lumen and is unable to block conductance effectively.

Precisely how the Phe clamp interacts with substrate polypeptides to foster translocation remains uncertain. However, the clamp was found to be the major conductance-blocking site for certain hydrophobic drugs and hydrophobic model cations, such as tetrabutylammonium (TBA) ions (90–92). For

example, the affinity of TBA for Phe427Ala channels relative to wild-type channels was reduced by a factor of 4000, and the affinity of the polyaromatic, 4-aminoquinolone drug, quinacrine (93), was reduced by 1000 (18). Examination of a library of 35 quaternary ammonium and phosphonium ion compounds led to the conclusion that the Phe clamp does not recognize specific geometric or steric features of the substrates. Instead, it appears to recognize compounds primarily by nonspecific hydrophobic interactions, although its π -electron clouds may contribute electrostatically through aromatic-aromatic, π - π , and cation- π interactions.

The characteristics of the Phe clamp in interacting with small molecules, combined with the fact that substrate polypeptides must unfold in order to be translocated, are consistent with a chaperone-like function in which the clamp's phenyl rings interact primarily with exposed hydrophobically dense segments of the substrate polypeptides (18). In LF and EF, as is true for globular proteins in general, hydrophobically dense segments occur periodically along the chain. As the molten globular substrate protein undergoes transient unfolding and is drawn incrementally into the channel, such hydrophobic segments would be expected to bind favorably to the Phe clamp and thus to pause. However, given that the Phe clamp site actually catalyzes translocation, it must reduce some other energy bar-

rier, such as unfolding of the substrate protein. In essence, the Phe clamp site may create an environment that mimics the hydrophobic core of the unfolding molten globular protein. Transient interaction of hydrophobic segments of the translocating polypeptide with the Phe clamp would reduce the energy penalty of exposing hydrophobic side chains to the solvent or the hydrophilic lumen of the channel.

Alternatively, the Phe clamp may function primarily to form a seal around the translocating polypeptide, blocking the passage of ions, as shown in single-channel conductance experiments (18, 85). This seal would preserve the proton gradient across the membrane, at least in the microenvironment of an individual pore, and thereby maintain this gradient as a potential energy source for driving translocation. It is conceivable that the Phe clamp serves both as a seal and a chaperonin. The Δ pH-driven charge-state ratchet may work in tandem with the Phe clamp, which has been proposed to be a hydrophobic ratchet.

In the final analysis, the PA₆₃ pore may be conceived to function as an enzyme, with the substrates being LF and EF bound at the pore entrance in the endosome, the products being these proteins delivered to the cytosol, the active site being the Phe clamp, and the driving force being the transmembrane pH gradient. In a sense, the pore functions as a proton/protein symporter.

SUMMARY POINTS

1. Pathogenic bacteria have evolved a number of systems to deliver harmful enzymes into host cells. The tripartite anthrax toxin is one of the most tractable of such systems for study of the entry process.
2. Entry begins when the pore-forming component, protective antigen (PA), binds to a cellular receptor (ANTXR1 or ANTXR2), is proteolytically activated, and oligomerizes to form a ring-shaped heptamer, called the prepore (**Figure 1**). The prepore binds one or both of the two enzymatic components, lethal factor (LF) or edema factor (EF), and the resulting complexes are trafficked to the endosome. There, under the influence of acidic pH, the prepore forms a transmembrane pore, and LF and EF unfold and cross the endosomal membrane via the pore to the cytosol.

3. The pore is believed to have a mushroom shape, with a globular cap, where LF and EF bind via their N-terminal domains, and a 14-strand transmembrane β -barrel formed by the interaction of 7 β -hairpins from domains 2 of the heptamer.
4. Both receptors, ANTXR1 and ANTXR2, have a VWA/I domain which binds PA. Contacts involve the domain 2 of PA as well as its canonical receptor-binding domain (domain 4). ANTXR2 binds PA more tightly than ANTXR1, and a lower pH is required for pore formation when the prepore is bound to the former.
5. PA forms cation-selective pores in planar phospholipid bilayers in the absence of receptors. The translocation of LF/EF through these pores can be replicated in this system under conditions close to those in the endosome.
6. When LF (or EF) binds the pore in the planar bilayer system, its flexible positively charged N terminus enters, blocking ion conductance and initiating an N- to C-terminal translocation process. Translocation is driven largely by a transmembrane proton gradient, from an acidic compartment (the endosome) to a neutral or less acidic one (the cytosol).
7. Rather than serving as a passive, water-filled conduit, the PA pore plays an active role in translocating LF and EF. The seven Phe427 side chains within the lumen of the pore form a structure called the Phe clamp, which is required for protein translocation through the pore. The Phe clamp may perform either or both of two functions: i) by forming a seal around the translocating polypeptide, it may prevent ion passage and thereby preserve the force-generating proton gradient; ii) by transiently binding hydrophobic segments of the translocating polypeptide, it may reduce the energy barrier to unfolding of the translocating polypeptide.
8. Translocation of LF and EF through the PA pore is proposed to occur by a charge-state Brownian ratchet mechanism. Because the pore excludes negatively charged segments of polypeptide, acidic residues can enter only after being protonated in the endosome (low pH). After they reach the cytosol (neutral pH), these segments are then rapidly deprotonated and cannot back diffuse into the pore. This results in a directionally biased diffusion through the pore by the translocating protein.

FUTURE ISSUES

1. Structure of the PA pore. Although crystallographic structures of monomeric PA, LF and EF, the prepore, and the ANTXR2-bound forms of monomeric PA and the prepore are known, direct structural information about the pore is lacking. Because the pore is an integral membrane protein, crystallization is a major challenge.
2. Does the pore remain associated with receptor? The PA prepore can form pores in planar phospholipid bilayers, indicating that pore formation is not dependent on receptors or other cellular proteins, and there is evidence from studies in cells that the receptor dissociates once the pore is formed. Nonetheless questions remain about the possible retention of interaction of the pore with receptors or other cellular proteins.

3. Are cellular chaperones involved in the unfolding, translocation and/or refolding of LF and EF? Although the translocation process can be replicated in planar phospholipid bilayers, it is conceivable that cellular chaperones may aid in this process in vivo. Results from studies in isolated endosomes have suggested that Hsp90 is involved in the translocation and/or refolding of diphtheria toxin, which also enters the cytosol from endosomes (94).
4. Can a single PA pore translocate more than one bound molecule of LF and/or EF after it enters the endosome? The efficiency of translocation in vivo is in need of further study.

DISCLOSURE STATEMENT

Both authors hold stock in PharmAthene, Inc. R.J. Collier is a consultant for a company that may develop drug treatments for anthrax.

ACKNOWLEDGMENTS

We thank John Naughton for help in preparing the figures. Our experimental research on anthrax toxin and its receptors has been supported by grants from the National Institute of Allergy and Infectious Diseases (AI22021, AI84849, and AI56013). This review was written in part while one of us (R.J.C.) was a guest in the laboratory of Prof. Klaus Aktories at the University of Freiburg, working under a Research Award from the Alexander von Humboldt Foundation.

LITERATURE CITED

1. Abrami L, Reig N, van der Goot FG. 2005. *Trends Microbiol.* 13:72–78
2. Agrawal A, Pulendran B. 2004. *Cell Mol. Life Sci.* 61:2859–65
3. Collier RJ, Young JA. 2003. *Annu. Rev. Cell Dev. Biol.* 19:45–70
4. Moayeri M, Leppla SH. 2004. *Curr. Opin. Microbiol.* 7:19–24
5. Mock M, Fouet A. 2001. *Annu. Rev. Microbiol.* 55:647–71
6. Scobie HM, Young JA. 2005. *Curr. Opin. Microbiol.* 8:106–12
7. Barth H, Aktories K, Popoff MR, Stiles BG. 2004. *Microbiol. Mol. Biol. Rev.* 68:373–402
8. Duesbery NS, Webb CP, Leppla SH, Gordon VM, Klimpel KR, et al. 1998. *Science* 280:734–37
9. Vitale G, Pellizzari R, Recchi C, Napolitani G, Mock M, Montecucco C. 1998. *Biochem. Biophys. Res. Commun.* 248:706–11
10. Leppla SH. 1982. *Proc. Natl. Acad. Sci. USA* 79:3162–66
11. Petosa C, Collier RJ, Klimpel KR, Leppla SH, Liddington RC. 1997. *Nature* 385:833–38
12. Lacy DB, Wigelsworth DJ, Melnyk RA, Harrison SC, Collier RJ. 2004. *Proc. Natl. Acad. Sci. USA* 101:13147–51
13. Santelli E, Bankston LA, Leppla SH, Liddington RC. 2004. *Nature* 430:905–8
14. Benson EL, Huynh PD, Finkelstein A, Collier RJ. 1998. *Biochemistry* 37:3941–48
15. Qa'dan M, Christensen KA, Zhang L, Roberts TM, Collier RJ. 2005. *Mol. Cell Biol.* 25:5492–98
16. Mogridge J, Mourez M, Collier RJ. 2001. *J. Bacteriol.* 183:2111–16

17. Rosovitz MJ, Schuck P, Varughese M, Chopra AP, Mehra V, et al. 2003. *J. Biol. Chem.* 278:30936–44
18. Krantz BA, Melnyk RA, Zhang S, Juris SJ, Lacy DB, et al. 2005. *Science* 309:777–81
19. Bradley KA, Mogridge J, Mourez M, Collier RJ, Young JA. 2001. *Nature* 414:225–29
20. Scobie HM, Rainey GJ, Bradley KA, Young JA. 2003. *Proc. Natl. Acad. Sci. USA* 100:5170–74
21. Liu S, Leppla SH. 2003. *J. Biol. Chem.* 278:5227–34
22. Rainey GJ, Wigelsworth DJ, Ryan PL, Scobie HM, Collier RJ, Young JA. 2005. *Proc. Natl. Acad. Sci. USA* 102:13278–83
23. Nanda A, Carson-Walter EB, Seaman S, Barber TD, Stampfl J, et al. 2004. *Cancer Res.* 64:817–20
24. Bell SE, Mavila A, Salazar R, Bayless KJ, Kanagala S, et al. 2001. *J. Cell Sci.* 114:2755–73
25. St Croix B, Rago C, Velculescu V, Traverso G, Romans KE, et al. 2000. *Science* 289:1197–202
26. Carson-Walter EB, Watkins DN, Nanda A, Vogelstein B, Kinzler KW, St Croix B. 2001. *Cancer Res.* 61:6649–55
27. Hotchkiss KA, Basile CM, Spring SC, Bonuccelli G, Lisanti MP, Terman BI. 2005. *Exp. Cell Res.* 305:133–44
28. Rmali KA, Al-Rawi MA, Parr C, Puntis MC, Jiang WG. 2004. *Int. J. Mol. Med.* 14:75–80
29. Bonuccelli G, Sotgia F, Frank PG, Williams TM, de Almeida CJ, et al. 2005. *Am. J. Physiol. Cell Physiol.* 288:C1402–10
30. Rmali KA, Puntis MC, Jiang WG. 2005. *Biochem. Biophys. Res. Commun.* 334:231–38
31. Hanks S, Adams S, Douglas J, Arbour L, Atherton DJ, et al. 2003. *Am. J. Hum. Genet.* 73:791–800
32. Dowling O, Difeo A, Ramirez MC, Tukul T, Narla G, et al. 2003. *Am. J. Hum. Genet.* 73:957–66
33. Wigelsworth DJ, Krantz BA, Christensen KA, Lacy DB, Juris SJ, Collier RJ. 2004. *J. Biol. Chem.* 279:23349–56
34. Lacy DB, Wigelsworth DJ, Scobie HM, Young JA, Collier RJ. 2004. *Proc. Natl. Acad. Sci. USA* 101:6367–72
35. Bradley KA, Mogridge J, Rainey GJA, Batty S, Young JAT. 2003. *J. Biol. Chem.* 278:49342–47
36. Shimaoka M, Takagi J, Springer TA. 2002. *Annu. Rev. Biophys. Biomol. Struct.* 31:485–516
37. Scobie HM, Wigelsworth DJ, Marlett JM, Thomas D, Rainey GJA, et al. 2006. *PLoS Pathog.* 2:949–55
38. Scobie HM, Thomas D, Marlett JM, Destito G, Wigelsworth DJ, et al. 2005. *J. Infect. Dis.* 192:1047–51
39. Ustinov VA, Plow EF. 2002. *J. Biol. Chem.* 277:18769–76
40. Klimpel KR, Molloy SS, Thomas G, Leppla SH. 1992. *Proc. Natl. Acad. Sci. USA* 89:10277–81
41. Molloy SS, Bresnahan PA, Leppla SH, Klimpel KR, Thomas G. 1992. *J. Biol. Chem.* 267:16396–402
42. Christensen KA, Krantz BA, Melnyk RA, Collier RJ. 2005. *Biochemistry* 44:1047–53
43. Gao-Sheridan S, Zhang S, Collier RJ. 2003. *Biochem. Biophys. Res. Commun.* 300:61–64
44. Milne JC, Furlong D, Hanna PC, Wall JS, Collier RJ. 1994. *J. Biol. Chem.* 269:20607–12
45. Christensen KA, Krantz BA, Collier RJ. 2006. *Biochemistry* 45:2380–86
46. Abrami L, Liu S, Cosson P, Leppla SH, van der Goot FG. 2003. *J. Cell Biol.* 160:321–28
47. Abrami L, Leppla SH, van der Goot FG. 2006. *J. Cell Biol.* 172:309–20

48. Beauregard KE, Collier RJ, Swanson JA. 2000. *Cell Microbiol.* 2:251–58
49. Elliott JL, Mogridge J, Collier RJ. 2000. *Biochemistry* 39:6706–13
50. Pimental RA, Christensen KA, Krantz BA, Collier RJ. 2004. *Biochem. Biophys. Res. Commun.* 322:258–62
51. Mogridge J, Cunningham K, Collier RJ. 2002. *Biochemistry* 41:1079–82
52. Mogridge J, Cunningham K, Lacy DB, Mourez M, Collier RJ. 2002. *Proc. Natl. Acad. Sci. USA* 99:7045–48
53. Cunningham K, Lacy DB, Mogridge J, Collier RJ. 2002. *Proc. Natl. Acad. Sci. USA* 99:7049–53
54. Ren G, Quispe J, Leppla SH, Mitra AK. 2004. *Structure* 12:2059–66
55. Lacy DB, Mourez M, Fouassier A, Collier RJ. 2002. *J. Biol. Chem.* 277:3006–10
56. Lacy DB, Lin HC, Melnyk RA, Schueler-Furman O, Reither L, et al. 2005. *Proc. Natl. Acad. Sci. USA* 102:16409–14
57. Melnyk RA, Hewitt KM, Lacy DB, Lin HC, Gessner CR, et al. 2006. *J. Biol. Chem.* 281:1630–35
58. Boll W, Ehrlich M, Collier RJ, Kirchhausen T. 2004. *Eur. J. Cell Biol.* 83:281–88
59. Wei W, Lu Q, Chaudry GJ, Leppla SH, Cohen SN. 2006. *Cell* 124:1141–54
60. He X, Semenov M, Tamai K, Zeng X. 2004. *Development* 131:1663–77
61. Santy LC, Casanova JE. 2002. *Curr. Biol.* 12:R360–62
62. Lu Q, Wei W, Kowalski PE, Chang AC, Cohen SN. 2004. *Proc. Natl. Acad. Sci. USA* 101:17246–51
63. Krauss M, Kinuta M, Wenk MR, De Camilli P, Takei K, Haucke V. 2003. *J. Cell Biol.* 162:113–24
64. Paleotti O, Macia E, Luton F, Klein S, Partisani M, et al. 2005. *J. Biol. Chem.* 280:21661–66
65. Abrami L, Lindsay M, Parton RG, Leppla SH, van der Goot FG. 2004. *J. Cell Biol.* 166:645–51
66. Maxfield FR, McGraw TE. 2004. *Nat. Rev. Mol. Cell Biol.* 5:121–32
67. Blaustein RO, Koehler TM, Collier RJ, Finkelstein A. 1989. *Proc. Natl. Acad. Sci. USA* 86:2209–13
68. Koehler TM, Collier RJ. 1991. *Mol. Microbiol.* 5:1501–6
69. Milne JC, Collier RJ. 1993. *Mol. Microbiol.* 10:647–53
70. Wesche J, Elliott JL, Falnes PO, Olsnes S, Collier RJ. 1998. *Biochemistry* 37:15737–46
71. Sun J, Vernier G, Wigelsworth DJ, Collier RJ. 2007. *J. Biol. Chem.* 282:1059–65
72. Nassi S, Collier RJ, Finkelstein A. 2002. *Biochemistry* 41:1445–50
73. Nguyen TL. 2004. *J. Biomol. Struct. Dyn.* 22:253–65
74. Wolfe JT, Krantz BA, Rainey GJ, Young JA, Collier RJ. 2005. *J. Biol. Chem.* 280:39417–22
75. Sellman BR, Nassi S, Collier RJ. 2001. *J. Biol. Chem.* 276:8371–76
76. Mourez M, Yan M, Lacy DB, Dillon L, Bentsen L, et al. 2003. *Proc. Natl. Acad. Sci. USA* 100:13803–8
77. Sellman BR, Mourez M, Collier RJ. 2001. *Science* 292:695–97
78. Yan M, Collier RJ. 2003. *Mol. Med.* 9:46–51
79. Krantz BA, Trivedi AD, Cunningham K, Christensen KA, Collier RJ. 2004. *J. Mol. Biol.* 344:739–56
80. Pannifer AD, Wong TY, Schwarzenbacher R, Rensus M, Petosa C, et al. 2001. *Nature* 414:229–33
81. Zhang S, Finkelstein A, Collier RJ. 2004. *Proc. Natl. Acad. Sci. USA* 101:16756–61
82. Blanke SR, Milne JC, Benson EL, Collier RJ. 1996. *Proc. Natl. Acad. Sci. USA* 93:8437–42
83. Neumeyer T, Tonello F, Dal Molin F, Schiffler B, Orlik F, Benz R. 2006. *Biochemistry* 45:3060–68

84. Zhang S, Udho E, Wu Z, Collier RJ, Finkelstein A. 2004. *Biophys. J.* 87:3842–49
85. Krantz BA, Finkelstein A, Collier RJ. 2006. *J. Mol. Biol.* 355:968–79
86. Rybak SL, Lanni F, Murphy RF. 1997. *Biophys. J.* 73:674–87
87. Sonawane ND, Thiagarajah JR, Verkman AS. 2002. *J. Biol. Chem.* 277:5506–13
88. Van Dyke RW, Hornick CA, Belcher J, Scharschmidt BF, Havel RJ. 1985. *J. Biol. Chem.* 260:11021–26
89. Melnyk RA, Collier RJ. 2006. *Proc. Natl. Acad. Sci. USA* 103:9802–7
90. Blaustein RO, Finkelstein A. 1990. *J. Gen. Physiol.* 96:943–57
91. Blaustein RO, Finkelstein A. 1990. *J. Gen. Physiol.* 96:905–19
92. Blaustein RO, Lea EJ, Finkelstein A. 1990. *J. Gen. Physiol.* 96:921–42
93. Orlik F, Schiffler B, Benz R. 2005. *Biophys. J.* 88:1715–24
94. Ratts R, Zeng H, Berg EA, Blue C, McComb ME, et al. 2003. *J. Cell Biol.* 160:1139–50
95. Liu S, Leung HJ, Leppla SH. 2007. *Cell Microbiol.* 9:977–87
96. Chen KH, Liu S, Bankston LA, Liddington RC, Leppla SH. 2007. *J. Biol. Chem.* PMID: 17251181

NOTE ADDED IN PROOF

During the final preparation of this review, the key role of receptor residue Tyr119 in regulating the PH threshold of toxin pore formation was also confirmed by another group (95). In addition, other receptor-specific PA variants were described (96).



Contents

Mitochondrial Theme

The Magic Garden <i>Gottfried Schatz</i>	673
DNA Replication and Transcription in Mammalian Mitochondria <i>Maria Falkenberg, Nils-Göran Larsson, and Claes M. Gustafsson</i>	679
Mitochondrial-Nuclear Communications <i>Michael T. Ryan and Nicholas J. Hoogenraad</i>	701
Translocation of Proteins into Mitochondria <i>Walter Neupert and Johannes M. Herrmann</i>	723
The Machines that Divide and Fuse Mitochondria <i>Suzanne Hoppins, Laura Lackner, and Jodi Nunnari</i>	751
Why Do We Still Have a Maternally Inherited Mitochondrial DNA? Insights from Evolutionary Medicine <i>Douglas C. Wallace</i>	781
Molecular Mechanisms of Antibody Somatic Hypermutation <i>Javier M. Di Noia and Michael S. Neuberger</i>	1
Structure and Mechanism of Helicases and Nucleic Acid Translocases <i>Martin R. Singleton, Mark S. Dillingham, and Dale B. Wigley</i>	23
The Nonsense-Mediated Decay RNA Surveillance Pathway <i>Yao-Fu Chang, J. Saadi Imam, Miles F. Wilkinson</i>	51
Functions of Site-Specific Histone Acetylation and Deacetylation <i>Mona D. Shabbazian and Michael Grunstein</i>	75
The tmRNA System for Translational Surveillance and Ribosome Rescue <i>Sean D. Moore and Robert T. Sauer</i>	101
Membrane Protein Structure: Prediction versus Reality <i>Arne Elofsson and Gunnar von Heijne</i>	125

Structure and Function of Toll Receptors and Their Ligands <i>Nicholas J. Gay and Monique Gangloff</i>	141
The Role of Mass Spectrometry in Structure Elucidation of Dynamic Protein Complexes <i>Michal Sharon and Carol V. Robinson</i>	167
Structure and Mechanism of the 6-Deoxyerythronolide B Synthase <i>Chaitan Khosla, Yinyan Tang, Alice Y. Chen, Nathan A. Schnarr, and David E. Cane</i>	195
The Biochemistry of Methane Oxidation <i>Amanda S. Hakemian and Amy C. Rosenzweig</i>	223
Anthrax Toxin: Receptor Binding, Internalization, Pore Formation, and Translocation <i>John A.T. Young and R. John Collier</i>	243
Synapses: Sites of Cell Recognition, Adhesion, and Functional Specification <i>Soichiro Yamada and W. James Nelson</i>	267
Lipid A Modification Systems in Gram-negative Bacteria <i>Christian R.H. Raetz, C. Michael Reynolds, M. Stephen Trent, and Russell E. Bishop</i>	295
Chemical Evolution as a Tool for Molecular Discovery <i>S. Jarrett Wrenn and Pebr B. Harbury</i>	331
Molecular Mechanisms of Magnetosome Formation <i>Arash Komeili</i>	351
Modulation of the Ryanodine Receptor and Intracellular Calcium <i>Ran Zalk, Stephan E. Lebnart, and Andrew R. Marks</i>	367
TRP Channels <i>Kartik Venkatachalam and Craig Montell</i>	387
Studying Individual Events in Biology <i>Stefan Wennmalm and Sanford M. Simon</i>	419
Signaling Pathways Downstream of Pattern-Recognition Receptors and Their Cross Talk <i>Myeong Sup Lee and Young-Joon Kim</i>	447
Biochemistry and Physiology of Cyclic Nucleotide Phosphodiesterases: Essential Components in Cyclic Nucleotide Signaling <i>Marco Conti and Joseph Beavo</i>	481
The Eyes Absent Family of Phosphotyrosine Phosphatases: Properties and Roles in Developmental Regulation of Transcription <i>Jennifer Jemc and Ilaria Rebay</i>	513

Assembly Dynamics of the Bacterial MinCDE System and Spatial Regulation of the Z Ring <i>Joe Lutkenhaus</i>	539
Structures and Functions of Yeast Kinetochore Complexes <i>Stefan Westermann, David G. Drubin, and Georjana Barnes</i>	563
Mechanism and Function of Formins in the Control of Actin Assembly <i>Bruce L. Goode and Michael J. Eck</i>	593
Unsolved Mysteries in Membrane Traffic <i>Suzanne R. Pfeffer</i>	629
Structural Biology of Nucleocytoplasmic Transport <i>Atlanta Cook, Fulvia Bono, Martin Jinek, and Elena Conti</i>	647
The Postsynaptic Architecture of Excitatory Synapses: A More Quantitative View <i>Morgan Sheng and Casper C. Hoogenraad</i>	823

Indexes

Cumulative Index of Contributing Authors, Volumes 72–76	849
Cumulative Index of Chapter Titles, Volumes 72–76	853

Errata

An online log of corrections to *Annual Review of Biochemistry* chapters (if any, 1997 to the present) may be found at <http://biochem.annualreviews.org/errata.shtml>